Three-Dimensional (3D) Polypyrrole Microstructures with High Aspect Ratios Fabricated by Localized Electropolymerization

Seung Kwon Seol,[†] Ji Tae Kim,[†] Jung Ho Je,*,[†] Yeukuang Hwu,[‡] and G. Margaritondo[§]

X-ray Imaging Center (XIC), Department of Materials Science and Engineering, Pohang University of Science and Technology, Pohang 790-784, Korea; Institute of Physics, Academia Sinica, 128 Academia Rd, sec. 2, Nankang, Taipei 11529, Taiwan; and Faculté des Sciences de Base, Ecole Polytechnique Fédérale, CH-1015 Lausanne, Switzerland

ABSTRACT: We present the three-dimensional (3D) growth of polypyrrole (PPy) microstructures with high aspect ratios (HAR) by a localized electropolymerization. The radicals formed by an oxidation of Py monomer is localized on the targeting area due to a confinement of electric field, forming a PPy structure. We found that a reversal point at which the relative field strengths of E_c (center of the grown structure) and E_e (edge) are reversed is a critical factor in determining the growth characteristic of the 3D PPy structure. A porous structure with open and closed pores is produced below the reversal point by the hydrogen bubble trapping in a gap between the microelectrode and the grown structure. Above the reversal point, a structure with dense and uniform features is obtained by a steady supply of monomer in the gap without bubble trapping.

I. Introduction

Conducting polymers such as polyaniline (PANI) and polypyrrole (PPy) are interesting materials for diverse applications due to their electrical properties, mechanical flexibility, volume-changing properties, and relatively low production cost.[1–3] Their practical applications often require the production of patterned structures in micrometer and submicrometer length scales. Traditionally, such patterns were achieved with lithographic methods such as photo-, electron-, or ion beam lithography.[4,5] However, these methods may induce damage and involve high costs. To meet these challenges, area-selective electropolymerization approaches by patterned SAMs (self-assembled monolayers) and soft lithography—micromolding in capillaries (MIMIC) and microcontact printing (μCP)—were developed.[6,7]

However, most of these methods are limited to the 2D patterning of thin polymer films. The fabrication of the 3D conducting polymer structures with high aspect ratios (HAR) remains a challenge. Such structures are particularly important in view of a broad range of device applications in microelectronics, biomedical devices, and microsystems such as actuators and sensors.

Here, we report on the growth of three-dimensional (3D) polypyrrole (PPy) microstructures with high aspect ratios (HAR), based on a novel strategy using localized electropolymerization. The generation of radical cations is localized to a targeting area by a confinement of electric field, enabling us to fabricate HAR (over 50:1) structures with different geometries—from simple straight lines to structures with complex features.

A schematic illustration of the localized electropolymerization method is shown in Scheme 1. By applying an electrostatic potential across a very small gap separating a microelectrode and a substrate, the generation of radicals induced by Py monomer oxidation is confined in the gap.[8–11] The polymerization caused by the oxidation reaction of the radicals with the other monomers in solution is then localized to a small area on the substrate, resulting in a synthesis of a PPy microstructure

Scheme 1. Schematic Illustration of Localized Electropolymerization of a Polypyrrole (PPy) Structure[a]
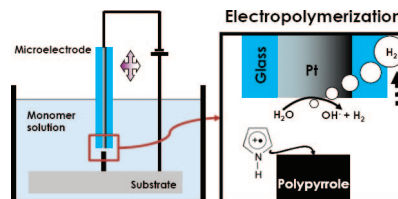
[a] The concept of localized electropolymerization is illustrated on the right-hand side. Hydrolysis reactions at the microelectrode produce hydrogen bubbles.

protruding toward the microelectrode. In parallel, hydrogen bubbles are generated on the microelectrode by hydrolysis.

II. Experimental Section

We fabricated by localized electropolymerization PPy structures at room temperature using 0.7 M Py and 0.2 M H_2SO_4. A microelectrode with 50 μm diameter was prepared by sealing Pt wire (99.95%, Alfa Aesar) in a glass tube and then polishing the surface. Platinum-coated silicon wafers were used as substrates. The microelectrode position was accurately controlled by three stepping motors.

The experiments were performed at the "7B2 X-ray Microscopy" beamline of the Pohang Light Source (PLS), Korea.[12] Field emission scanning electron microscopy (FE-SEM, JEOL JSM6330F) was additionally used to study the microscopic characteristics of the grown structures. The microradiographic monitoring of the growth process was implemented in situ in a specially designed miniature solution bath machined from a Teflon block and sealed by Kapton films that were X-ray transparent and stable for most chemical reactions. The distance between the two cell windows was optimized to ~5 mm to avoid unnecessary X-ray absorption by the monomer solution. For microtomography, the grown structure was mounted on a translation/rotation stage with precise positioning (250 nm/0.002°), and 1000 projection radiographs were taken while rotating the sample between 0° and 180°. Slice images were then reconstructed by using a self-developed reconstruction algorithm.[13,14]

* Corresponding author. E-mail: jhje@postech.ac.kr.
[†] Pohang University of Science and Technology.
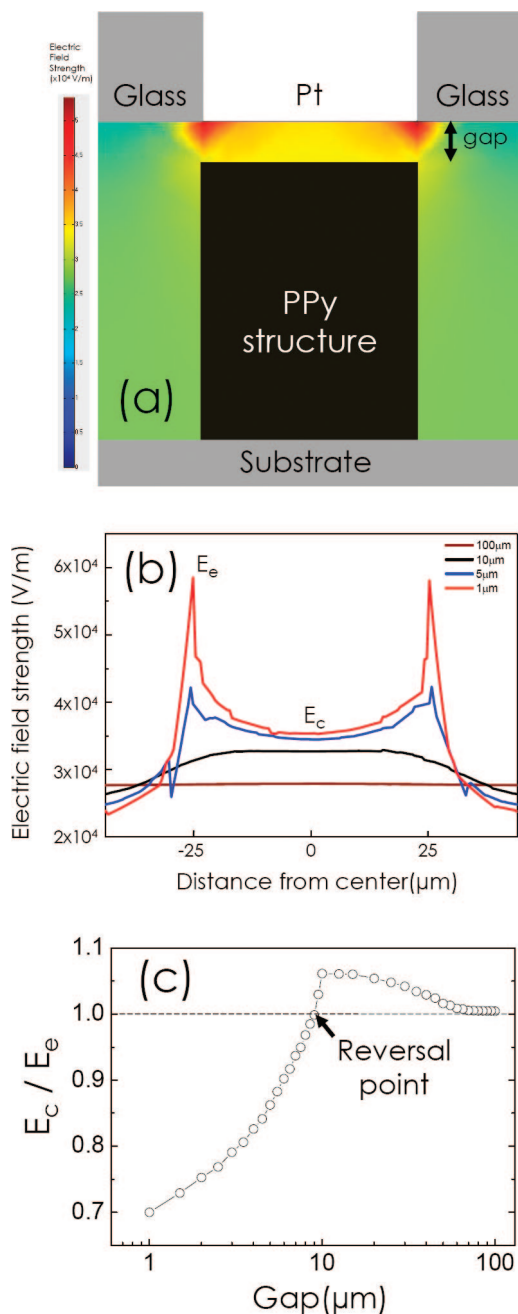[‡] Academia Sinica.
[§] Ecole Polytechnique Fédérale.

Figure 1. (a) Distribution of the electric field strength on the grown structure in a microelectrode (structure gap of ∼10 μm). (b) Profiles of transverse electric field strength distribution on the grown structure for 1, 5, 10, and 100 μm gap widths. (c) Gap-dependent variation of the field strength ratio (E_c/E_e). Note the "reversal point" for which E_c becomes larger than E_e.

III. Results and Discussion

The grown microstructure can be significantly affected by the electric field distribution, taking into account the very small gap (less than 100 μm) between the microelectrode and the grown structure. We thus begin our discussion from the distribution of the electric field strength on the grown structure during the PPy growth. Figure 1a shows a simulation diagram of the electric field strength distribution in the gap with 10 μm at an applied voltage of 4.5 V. Figure 1b illustrates the profile of the transverse field strength distribution for a gap width of 1, 5, 10, and 100 μm. At relatively large gap widths (≥10 μm), the field strength exhibits a maximum value at the center of the grown structure. As the gap decreases from 100 to 10 μm, the localization of the electric field near the center is further

enhanced. In contrast, the maximum field shifts from the center to the edge due to the edge enhancement at relatively small gap widths (≤5 μm). As the gap decreases from 5 to 1 μm, the effect of the edge enhancement further increases.

To compare the two electric field strengths on the center (E_c) and the edge (E_e) of the grown structure, we plot in Figure 1c the strength ratio, E_c/E_e, as a function of the gap. As the gap decreases from 100 to 10 μm, the ratio gradually increases, indicating an enhancement of the local electric field at the center. (At 100 μm, the localization of the field at the center is very weak.) As the gap further decreases below 10 μm, the ratio begins to decrease, reaching the value of 1 at 9.2 μm. Below this point, E_e becomes larger than E_c, shifting the position of the maximum field strength from the center to the edge. This point is called in the following the "reversal point".

We will now discuss the effect of the electric field strength on the growth characteristic of the PPy structure. The growth evolution was studied using real-time synchrotron X-ray microradiography.[15–18] Figure 2a,b shows the radiographic images of the PPy structure grown with an initial gap of 50 μm and a constant applied voltage of 4.5 V. The gap continuously decreases during the PPy growth due to the fixed position of the microelectrode. Until the gap decreases to 9 μm, PPy grows as a rod shape with a convex top (Figure 2a) because of the field strength at the center. (The black thick curved line in the image is from a bubble attached on the Kapton window in the electrochemical bath and not related to the PPy structure.) As the gap decreases to 4 μm, the rod shape changes to a concave top as shown in Figure 2b.

This shape change is due to a reversal of the relative field strengths of E_c and E_e (see Figure 1c). In order to explain the growth evolution in detail, we measured the curvature of the top of the rod from the radiographic image during the growth and plotted the curvature radius as a function of the field strength ratio (E_c/E_e) in Figure 2c. Above the reversal point (zone I), the radius sign is positive with a convex top, as illustrated by R_1 in the inset of Figure 2c, and its value is almost constant. Such convex top is due to a strong localization of the electric field at the center, inducing a high concentration of radicals. On the other hand, as the strength ratio decreases below the reversal point, the radius sign, illustrated by R_2 in the inset of Figure 2c, suddenly changes to negative corresponding to a concave top (zone III), after going through a transition zone (zone II). The period of the transition zone is very short, less than 0.4 s, as can be seen in Figure 2d. The change of the curvature radius is due to the edge enhancement of the electric field on the rod edge, inducing a high concentration of radicals near the edge. The transition from the zone I to the zone III leads to a slight increase of the curvature radius in the transition zone II. These results illustrate the importance of the reversal point in determining the morphology of structures grown by the localized electropolymerization.

We tested the PPy growth in the two conditions of zone I and zone III. The continuous growth in zone I or zone III requires keeping the gap constant during the entire process. The constant gap was achieved by monitoring the grown structure using the real-time X-ray microradiography in situ and by adjusting the microelectrode height.

The first test (zone I) was carried out at 4.5 V, keeping the gap to 10 μm. The resulting structure exhibits a smooth surface as seen in the FESEM image of Figure 3a. The internal structure, as shown by the tomographic slice in the inset of Figure 3a, reveals a very dense and smooth morphology.

The second test (zone III) was performed at 4.5 V, keeping the gap at 4 μm. Contrary to the growth morphology for zone I, a porous structure with a rough surface was obtained as shown in the FESEM image of Figure 3b. The internal structure, as
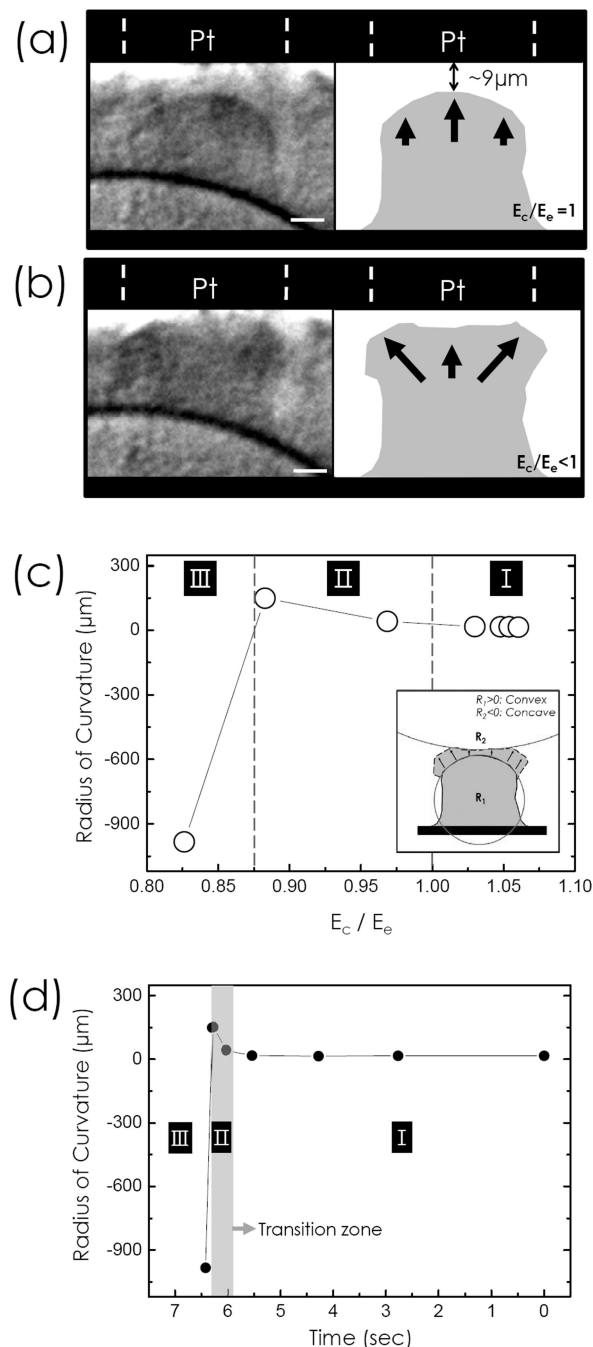
Figure 2. (a, b) Real-time X-ray radiographic images of the PPy growth process for an initial gap of 50 μm and an applied voltage of 4.5 V: (a) Until the gap decreases to 9 μm, PPy grows as a rod shape with a convex top. (b) At 4 μm, the rod top changes to concave (the grown structures are sketched on the right-hand side; scale bar: 10 μm). (c) Plot of the curvature radius of the top as a function of the field strength ratio (E_c/E_e) reveals three different zones. The inset illustrates the convex and the concave tops. (d) Variation of the curvature radius of the top with the growth time.

Figure 3. (a, b) FESEM images of PPy structures grown with an applied voltage of 4.5 V: (a) In zone I (above the reversal point ($\sim$10 μm gap)), the PPy structure is dense and smooth. The tomographic slice in the inset also reveals a very dense and smooth internal structure. (b) A PPy structure grown in zone III shows a porous morphology with many pits. The tomographic slice exhibits closed pores (black arrows) and an irregular perimeter with pits (white arrows) corresponding to open pores. (c, d) Microradiographic images for the growth process of the porous structure in (b): hydrogen bubbles generated on the microelectrode (marked by white and black arrows) are trapped in the closed space between the electrode and the concave surface of the PPy structure, producing a porous morphology with both open and closed pores (the grown structures are sketched at the bottom; scale bar: 25 μm).

shown by the tomographic slice in the inset of Figure 3b, exhibits not only open (white arrows) but also closed pores (black arrows). The cause of the pore formation is that the hydrogen bubbles generated on the microelectrode by hydrolysis are trapped in the gap. The two consecutive microradiographic images in Figure 3c,d show the formation of a closed pore (marked by a white arrow). Hydrogen bubbles confined in the closed space between the electrode and the concave surface of the PPy structure can be easily trapped, forming indeed closed pores, whereas the bubbles can easily escape from the gap
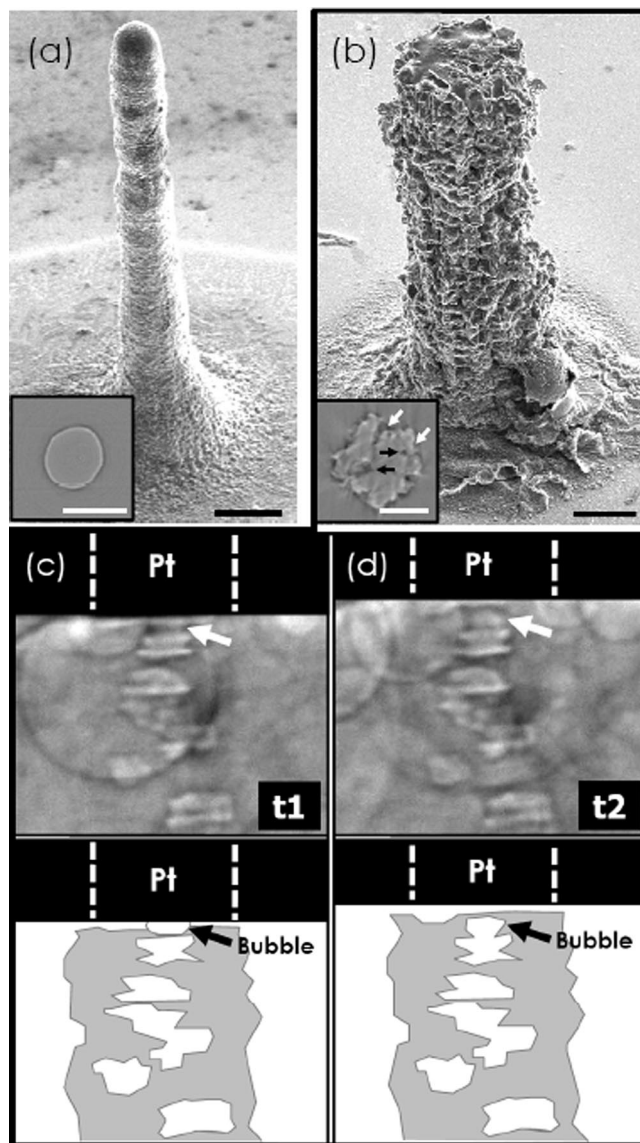
because of the convex surface of the grown structure in the zone I. The bubble trapping that also occurs on the periphery of the structure due to the extremely reduced gap and rapid PPy growth on the edge causes not only the formation of open pores but also an irregular and rough growth on the side by hindering the monomer supply.

The above results suggest that the continuous PPy growth in zone I leads to HAR structures with dense and smooth features. Figure 4 shows several additional successful fabrication tests of free-standing PPy HAR microstructures with different shapes in zone I ($E_c/E_e > 1$) with $\sim$10 μm gap: straight (a), zigzag (b), and a complex geometry (c).
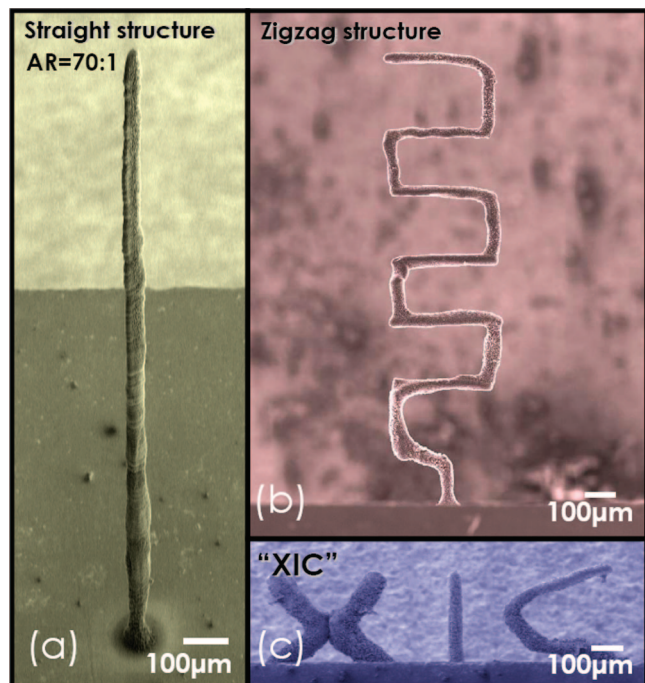
Figure 4. (a) FESEM images of free-standing PPy HAR microstructures with dense and smooth morphology. The images show (a) a wirelike straight structure with aspect ratio = 70, (b) a zigzag structure, and (c) a complex structure corresponding to the letters "XIC".

In summary, three-dimensional (3D) PPy HAR microstructures with high density and high uniformity were successfully fabricated by localized electropolymerization. We found that the reversal point at which the relative field strengths of E_c and E_e are reversed is a critical factor in determining the growth characteristic of the PPy structure. The porous morphology produced below the reversal point (zone III) is due to the hydrogen bubble trapping. Above the reversal point (zone I), a steady supply of monomer occurs in the gap without bubble trapping, producing a structure with dense and uniform features.

This localized electropolymerization approach is a simple, inexpensive, damage-free method, virtually without limitations on the thickness of the patterned structures. Furthermore, it is quite effective in producing conducting polymers doped with appropriate counterions. The practical cases presented here are only a few of the many different examples of conducting polymer HAR structures that our novel approach can fabricate by appropriate tuning of the growth parameters.

References and Notes

(1) MacDiarmid, A. G. *Angew. Chem., Int. Ed.* **2001**, *40*, 2581.
(2) Gustafsson, G.; Cao, Y.; Treacy, G. M.; Klavetter, F.; Colaneri, N.; Heeger, A. J. *Nature (London)* **1992**, *357*, 477.
(3) Jager, E. W. H.; Smela, E.; Inganas, O. *Science* **2000**, *290*, 1540.
(4) Renak, M. L.; Bazan, G. C.; Reitman, D. *Adv. Mater.* **1997**, *9*, 392.
(5) Hikmet, R. A. M.; Thomassen, R. *Adv. Mater.* **2003**, *15*, 115.
(6) Beh, W. S.; Kim, I. T.; Qin, D.; Xia, Y.; Whitesides, G. M. *Adv. Mater.* **1999**, *11*, 1038.
(7) Burdinski, D.; Saalmink, M.; van den Berg, J. P. W. G.; van der Marel, C. *Angew. Chem., Int. Ed.* **2006**, *45*, 4355.
(8) Asavapiriyanont, S.; Chandler, G. K.; Gunawardena, G. A.; Pletcher, D. *J. Electroanal. Chem.* **1984**, *177*, 229.
(9) Fermin, D. J.; Scharifker, B. R. *J. Electroanal. Chem.* **1993**, *357*, 273.
(10) Sadki, S.; Schottland, P.; Brodie, N.; Sabouraud, G. *Chem. Soc. Rev.* **2000**, *29*, 283.
(11) Hwang, B. J.; Santhanam, R.; Lin, Y.-L. *J. Electrochem. Soc.* **2000**, *147*, 2252.
(12) Baik, S.; Kim, H. S.; Jeong, M. H.; Lee, C. S.; Je, J. H.; Hwu, Y.; Margaritondo, G. *Rev. Sci. Instrum.* **2004**, *75*, 4355.
(13) Hwu, Y.; Je, J. H.; Margaritondo, G. *Nucl. Instrum. Methods Phys. Res., Sect. A* **2005**, *551*, 108.
(14) Pyun, A.; Bell, J. R.; Won, K. H.; Weon, B. M.; Seol, S. K.; Je, J. H.; Macosko, C. W. *Macromolecules* **2007**, *40*, 2029.
(15) Hwu, Y.; Tsai, W.-L.; Groso, A.; Margaritondo, G.; Je, J. H. *J. Phys. D: Appl. Phys.* **2002**, *35*, R105.
(16) Tsai, W. L.; Hsu, P. C.; Hwu, Y.; Chen, C. H.; Chang, L. W.; Je, J. H.; Lin, H. M.; Groso, A.; Margaritondo, G. *Nature (London)* **2002**, *417*, 139.
(17) Tsai, W. L.; Hsu, P. C.; Hwu, Y.; Chen, C. H.; Chang, L. W.; Je, J. H.; Margaritondo, G. *Nucl. Instrum. Methods Phys. Res., Sect. B* **2003**, *199*, 451.
(18) Seol, S.-K.; Pyun, A.; Hwu, Y.; Margaritondo, G.; Je, J.-H. *Adv. Funct. Mater.* **2005**, *15*, 934.